Solar Engineering — 1998
ASME 1998

SOLAR DISTILLATOR USING HUMID-AIR AND HEAT PIPES FOR RURAL AREAS IN MÉXICO

Ignacio R. Martín-Domínguez
Centro de Investigación en Materiales Avanzados
Miguel de Cervantes 120 Complejo Industrial
Chihuahua. 31109 Chihuahua, Chih. México
Ph.: (14) 39-1147 FAX: (14) 39-1112
imartin@mail.cimav.edu.mx

José A. Pérez-Galindo
Instituto Tecnológico de Durango
Departamento de Metal Mecánica
Felipe Pescador 1830 Ote.
34080 Durango, Dgo. México
Ph (18)18-5586 x 126 FAX:(18)18-4813

Alejandra Martín-Domínguez **Martha P. Hansen-Rodríguez**
Instituto Mexicano de Tecnología del Agua. Subcoordinación de Potabilización
Paseo Cuauhnáhuac 8532 Progreso 62550 Jiutepec, Mor. México
Ph : (73) 19-4299 FAX : (73) 19-4381 almartin@chac.imta.mx

ABSTRACT

This work presents a novel design of a solar distillator to be used in rural areas. The thermodynamic analysis of the proposed system is presented and evaluations of its performance on the basis of heating alternatives are given. In order to optimize system design, calculations were performed by means of a simulator, whose main characteristics are described.

NOMENCLATURE

$\dot{Q}$	heat flow	kW
T	temperature	°C, K
h	specific enthalpy	kJ/kg
$\dot{m}$	mass flow rate	kg/s

Greek symbols

ϕ	relative humidity	%
ω	humidity ratio	kg_w / kg_a

Subscripts

a	dry air
c	condensate
dw	dew point
e	evaporator
f	saturated liquid
fg	vaporization
g	saturated vapor
i	imaginary condition in evaporator
s	brine, saturation
tot	total
w	water

INTRODUCTION

Diarrhea is an illness closely correlated to drinking water quality, and in México is one of the top 10 health problems. In México 16% of the population does not have formal drinking water systems. From these, 47% are located in rural areas. 70% of the population without potable water systems live in 90,000 villages of no more than 1,000 inhabitants. Water potabilization is accomplished by filtration and chlorination in medium size to large towns, but in rural areas this is neither technically nor economically possible. Supply and use of chlorine is difficult, expensive and risky for small communities and, in many places, the available water has a high content of dissolved salt, which makes the problem even worse. Since in México solar energy is abundant, this energy source is a natural candidate to be used for desalination and potabilization of water.

México has an extension of almost two million square kilometers, 67% of these are considered semi-arid to dessertic regions. While the mean annual precipitation is about 770 mm, the northern part of the country receives only about 500 mm (with some regions with less than 50 mm of water per year). On the other hand, some southeast regions receive from 2,000 mm to 5,000 mm. These numbers show large disparities in water availability across México, worsened by the fact that 60% of the population lives in the altiplano and the northern high plateau, where only 12% of the water resources are available. The water availability *per capita* in México is estimated in about 5,200 m^3, which is half of what is available in the USA, or 1/20 of Canada.

The amount of thermal energy required for desalination is about 100 times that required for pasteurization, and there also exist other cheaper disinfection options, therefore the use of solar thermal energy is only justified if the available water contains salts or if there exists no other disinfection means available in the location, as it usually happens in isolated rural areas in México.

There have been several attempts in México to use solar energy for desalination purposes since the 60's. The preferred type of solar distillator has been the solar still geometry which, because of its

simplicity, is suitable to be built with readily available materials and unskilled labor. From 1974 to 1977 sixteen French solar plants were installed in México, the average collector size was 90 m^2 for 15 of them, and the last one was of 15,000 m^2. Nowadays, none of these plants is operating, and most of them are abandoned.

This work presents a new design of a distillator, based on a humid-air cycle, in which the various processes to accomplish distillation are assumed to take place in separated devices.

In the traditional solar still distillator the heating and evaporation processes occur on the floor of the still, while condensation occurs under the glass surface. These places are not believed to be the best for the duty, especially the condensing section. The glass covering absorbs some of the solar radiation, most of the infrared radiation from the collector, and the latent heat of condensation, and has to dissipate all this energy to the surrounding external air by natural convection from an almost flat horizontal surface, what will take place normally trough relatively small heat transfer coefficients. All this causes the glass covering to operate at relatively high temperatures, and condensation occurs at such temperatures. Also, trickling water accumulated beneath the glass intercept solar energy, re-heating water that is already pure, rather than evaporating water from the brine pool below. Therefore, since the overall performance of the system would be limited by the least efficient process, and with the observations stated above in mind, it was decided to follow the approach of using separate devices to perform each process.

To avoid the use of vacuum and high temperatures, air was selected as the water carrying media in the apparatus. Thus, water extraction from the contaminated source is accomplished by circulating and humidifying dry air over water in an evaporation section, and purified water is extracted from the air in a condensation section by dehumidification. The condensation process is assumed to take place over finned heat pipes so that, since heat is to be rejected to the atmosphere and heat pipes transport heat very efficiently, the largest possible temperature difference between evaporation and condensation may be obtained.

A difference in the capacity to absorb water in the evaporation section by hot dry air (relative to water temperature) and cold dry air is to be expected. This is due to the fact that the mass and heat transfer potentials are in opposite directions in the former case and in the same direction in the latter. This postulated difference, not investigated heretofore, was evaluated by comparison of the effects of using the solar energy to heat either the water or the air.

The design process was divided in stages, and the design of the system has been based on computer simulations in order to optimize the analysis of the apparatus performance and to match component sizes easily and thoroughly. This work presents results of the first stage, where the thermodynamic processes were analyzed to obtain a preliminary evaluation of the design.

Inclusion of the heat and mass transfer mechanisms comprises the ongoing second stage of the work, which will allow system sizing and optimization. Finally, a scaled down model will be constructed and instrumented to experimentally validate the design in the third stage of the project.

APPARATUS

System Description

As shown in Fig. 1, the proposed system is comprised of two solar collectors, one for air and one for water, an evaporator, where dry air and water streams interact to produce humid air, a heat pipe

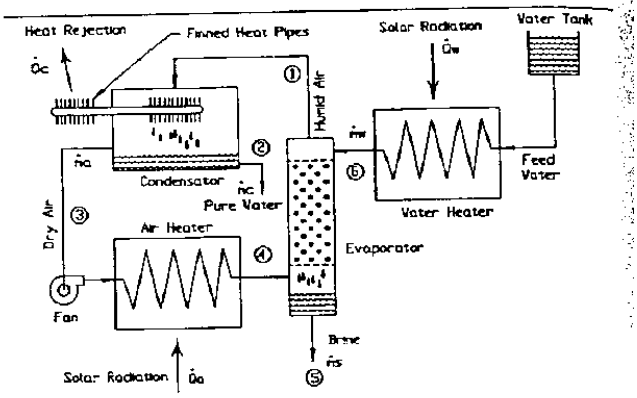

Figure 1. Proposed system

condenser, where the humid air is cooled as close to ambient temperature as possible to precipitate its humidity, and a photovoltaic power driven fan, to maintain the closed loop air circulation.

The reasons underlying component selection for the proposed design are the following:

- the system is to be used at locations where there are no other means to produce potable water.
- it should be able to operate unattended, use the smallest real state possible and produce drinking water from a variety of water sources, such as rivers, lakes, wells and others.
- the humid-air cycle was selected to avoid boiling and the use of vacuum while operating at atmospheric pressure.
- by using different devices to accomplish the cycle processes, it is possible to optimize the design of each device.
- the use of heat pipes makes it possible to maintain very low values of condensation temperatures, hopefully a few degrees above ambient temperature, thereby maximizing the temperature gradient between heat source and heat sink and the amount of condensate produced.

THERMODYNAMIC MODEL

The model of the system is based on energy and mass balances performed on each of the devices that conform the distillator. In this design the main objective is to vaporize as much water as possible in the packed tower, and to condensate it in the condenser. The operation of the packed tower is similar to a wet cooling tower, with the difference that here the objective is to evaporate as much water as possible, while in the cooling tower the purpose is to cool the water as much as possible. The wet cooling tower theory found in the literature cannot be directly applied to this problem, mainly because the effect of the vaporized water is normally neglected, but also because of the fact

possible, while in the cooling tower the purpose is to cool the water as much as possible. The wet cooling tower theory found in the literature cannot be directly applied to this problem, mainly because the effect of the vaporized water is normally neglected, but also because of the fact that the air is always assumed to be at less temperature than that of the entering water.

Condenser energy balance:

$$\dot{Q}_c = \dot{m}_a \left(h_1 - h_3 \right) - \dot{m}_c h_2 \quad (1)$$

Condenser mass balance:

$$\dot{m}_c = \dot{m}_a \left(\omega_1 - \omega_3 \right) \quad (2)$$

Since at this simulation stage the heat and mass transfer mechanisms were not included, to estimate the humid air conditions at the condenser exit it was assumed that the air is saturated after the condensation process, and that its temperature is 7°C above ambient temperature, which is reasonable if heat pipes are to be used in that equipment.

Solar collectors energy balances:

$$\dot{Q}_a = \dot{m}_a \left(h_4 - h_3 \right) \quad (3)$$

$$\dot{Q}_w = \dot{m}_w \left(h_6 - h_7 \right) \quad (4)$$

Evaporator analysis:

In the evaporator the air and water streams interchange heat and mass in a direct contact process. Since the air and water temperatures depend on the amount of heat supplied in the solar collectors and on

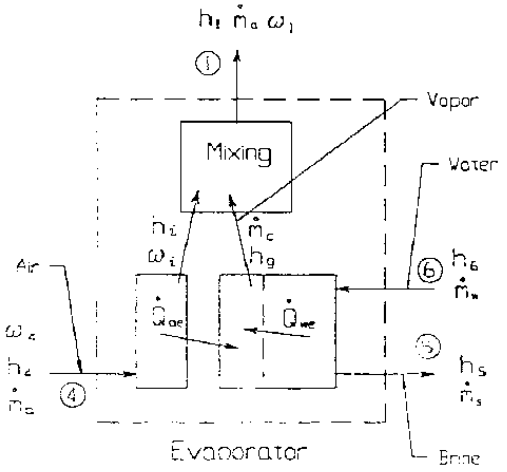

Figure 2. Evaporator control volume

their respective mass flow rates, and the governing heat and mass transfer phenomena varies according to their relative temperatures, exit conditions can not be obtained from energy and mass balances directly. To solve this problem, and based on film diffusion theory, Kern (1950), the evaporator analysis was divided into two imaginary sections, as shown in Fig. 2, the interface between water and humid air may receive energy from the air or the water and, since the objective of the system is to evaporate as much water as possible, the whole amount of available energy is assumed to be used for evaporation with no sensible heat exchanged between streams. Thereafter, the evaporated water is mixed with the air current to produce the final exit air stream.

When the air can provide energy (i.e. its temperature is greater than the inlet water temperature), its contribution to evaporation energy was calculated from:

$$\dot{Q}_{ae} = \dot{m}_a \left(h_4 - h_i \right) \quad (5)$$

where the subindex "i" refers to the imaginary conditions after the air supplied energy for water evaporation. The available energy from water for evaporation (when its inlet temperature is above that of the incoming air wet bulb temperature) was obtained from:

$$\dot{Q}_{we} = \dot{m}_w h_6 - \dot{m}_s h_5 \quad (6)$$

these two energy sources combine to produce an amount of evaporation (that equals the amount of condensate in the condenser) calculated with:

$$\dot{m}_c = \frac{\dot{Q}_{ae} + \dot{Q}_{we}}{h_g} \quad (7)$$

where the enthalpy is evaluated at the average temperature of conditions 5 and 6. Since condensate and brine flows are not known, equations 5, 6 and 7 have to be solved iteratively with the aid of the evaporator water mass balance:

$$\dot{m}_c = \dot{m}_a \left(\omega_1 - \omega_4 \right) = \dot{m}_w - \dot{m}_s \quad (8)$$

Finally, the evaporator exit enthalpy is obtained from an energy balance:

$$h_1 = \frac{\dot{m}_a h_i + \dot{m}_c h_g}{\dot{m}_a} \quad (9)$$

It should be noted that, due to the air enthalpy definition, h_1, h_i, and h_4 are air total enthalpies which include contributions from both the dry air and its water content. The air humidity balances, required to solve Eq. (9), are:

$$\omega_4 = \omega_i = \omega_1 - \frac{\dot{m}_c}{\dot{m}_a} \quad (10)$$

Thermodynamic limits and properties

The operating conditions of the system are limited by the temperature range between the atmospheric temperature (coldest location) and the exit temperatures of the solar collectors (hottest locations). In this study a constant value of 20°C was selected for the atmospheric temperature. If inexpensive common flat collectors are used, typical attainable temperatures are around 70°C and 85°C for water and air heating respectively. Arbitrarily, but including operation ranges above those for flat plate collectors, the temperature limits were set at 100°C for water and 150°C for air.

evaporator and the condenser ($\phi_1 = \phi_3 = 100$ %). The amount of water being transported between those devices will be directly proportional to the humidity ratio difference between these states ($\omega_1 > \omega_4$, $\omega_4 = \omega_3$), and the larger the temperature difference, the larger the amount of

- in a simulation run, one of the independent variables is permitted to vary between certain limits, while the other two take fixed values
- the fraction of heat power delivered to the water solar collector

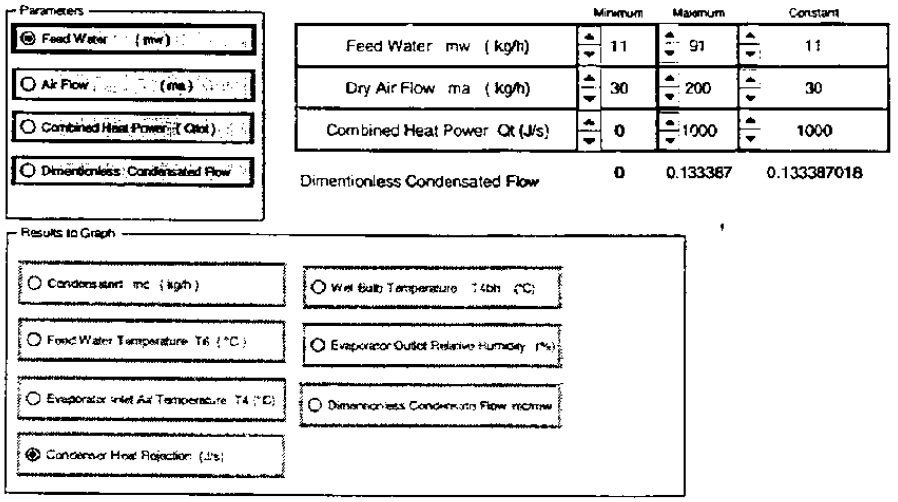

Figure 3. Graphic User Interface (GUI)

water transported. This fact highlights two of the design characteristics that should be considered as important, the condensate production rate depends on the temperature difference between evaporation and condensation, and also on the air flow rate. Nevertheless, those variables are not independent, therefore it is required to understand how they affect each other.

To calculate the different thermodynamic properties of water and humid air, correlations were obtained with data from ASHRAE (1985) and Çengel and Boles (1994). The equation-fitting was done by linear regression and the average deviation obtained was less than 0.1% over the complete data range. The curve-fitted properties were : enthalpies $h_f(T)$, $h_g(T)$, $h_{fg}(T)$, saturation pressure $P_s(T)$, saturation temperature $T_s(P)$, $T_s(h_f)$, dew point temperature $T_{dw}(\omega)$ and humidity ratio $\omega(T_{dw})$. Some of these correlations have already been published elsewhere, Martín-Domínguez (1993).

COMPUTER SIMULATION

To explore the performance of the proposed system under many different operation conditions with ease, a simulation program was developed. In this first stage of the project, only the thermodynamic analysis was incorporated.

The simulator was developed using an electronic spreadsheet which includes in its capabilities a high level structured programming language and programmable graphic controls. These, permitted to build a graphic user interface (GUI) whose basic characteristics are shown in Fig. 3.

The simulator main operational characteristics are:

- independent variables: feed water flow rate, air flow rate and total heat power supplied to the collectors
- is varied between 0 and 1 with 0.05 size increments, (the remaining fraction is delivered to the air solar collector), and a matrix of 231 operation conditions is calculated for 10 increments in the other independent variable
- a 3-D response surface is obtained
- the GUI permits the user to select the independent variable to be used in a run ("Parameter" on Fig. 3), to define the variation range for that variable and the fixed values for the other two independent variables (quick change cells to the right of "Parameter" on Fig. 3)
- the GUI also allows the selection of the calculated results to be displayed, choosing any one from a list of seven possible process variables, which includes: condensate flow rate (m_c), feed water temperature (T_6), hot air temperature (T_4), heat rejected on the condenser, hot air wet bulb temperature (T_{4bh}), humid air relative humidity, dimensionless condensate flow rate (m_c/m_w).

RESULTS

Figure 4 shows results of a typical simulation run for a given set of input parameters. In this example the feed water mass flow rate, m_w, was set at 11 kg/h, which was obtained from an estimate of the daily amount of water to be treated for a typical household of a Mexican rural area. Assuming a reasonable equipment size, with about two square meters of solar collector area, the total heat input to the system was estimated at 1000 W, on the basis of a solar insolation estimate of 500 W/m^2.

As mentioned before, one the main objectives of this work is to evaluate differences in the humidification process caused by the interaction of either hot dry air with cold water or of cold dry air with

hot water. On this basis, the fraction of total heat input to the water, Q_w/Q_{tot}, was selected to be the main independent variable, shown on the x axis, while the remaining heat was supposed to be used to heat the air.

Finally, as shown by each of the lines of Fig. 4, the air mass flow rate was used as a parameter. The range of variation shown in the figure was based on typical air/water mass flow rate ratios for humidifying systems of around 5 to 11, according to ASHRAE, 1992.

An overall examination of Fig. 4 shows that, for values of Q_w/Q_{tot} greater than 0.6, the amount of air fed into the system is relatively unimportant, since lines are very closely spaced, and the amount of evaporation, m_e, falls down linearly as the heat input to the water diminishes. It can also be seen that there are three distinct production modes which exist for any given air mass flow rate, as evidenced by the three values of the slope of m_e as a function of Q_w/Q_{tot}.

These observations may be explained by the model assumptions, made with the objective of maximizing the apparatus production under all operating conditions, and which will now be presented.

The most efficient use of the feed water energy occurs when it

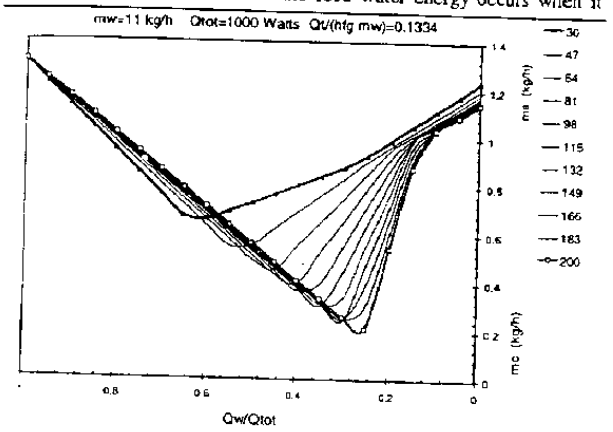

Figure 4. Condensate production

leaves a counter flow heat-mass exchanger (the humidifier) at the wet bulb temperature of the incoming air. This minimum possible exit temperature was calculated and used in the model unless the feed water temperature was lower than the aforementioned wet bulb temperature. Hence, in the former case, which corresponds to the two leftmost slopes in Fig. 4, the feed water contributes energy for the humidification process, while in the latter the water is assumed to leave at its entrance temperature and all of the evaporation energy must come from the air. This explains the linear change of m_e as a function of Q_w/Q_{tot} at the right extreme of the lines, since for a given air mass flow rate the energy input will be directly proportional to solar heat input.

From the standpoint of exit air temperature the most efficient process occurs when the air leaves at the highest possible value. This is due to the temperature-humidity relationship for humid air which, being a single-valued increasing function, implies higher values of humidity content when temperature increases. In the model, the evaporator exit air temperature was assumed to be equal to the feed water inlet temperature when this was higher, and was set at the wet bulb temperature otherwise.

The aforementioned assumptions may be used to explain the leftmost linear variation of the curves and the minimum values, since

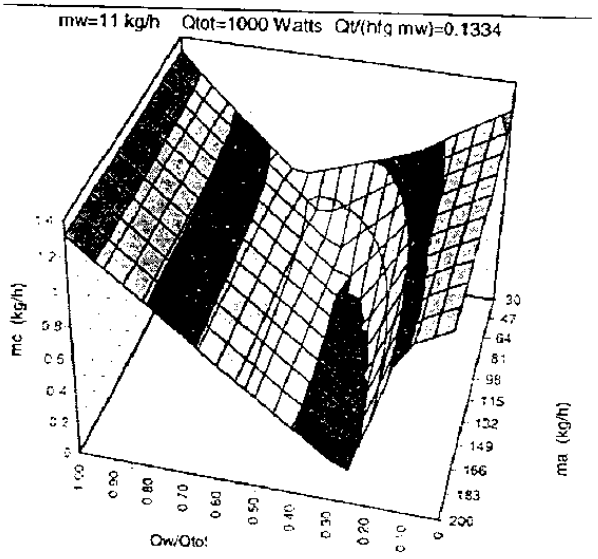

Figure 5. Condensate production (3-D)

in this region the feed water temperature is higher than that of the air. Hence, the energy required to heat and saturate the incoming air is fully supplied by the feed water energy content, which goes down as Q_w/Q_{tot} is lowered. The minimum production occurs when there are no sensible heat requirements, the air enters the evaporator at the same temperature of the feed water, and the energy supply is only used for water evaporation.

As Q_w/Q_{tot} continues to decrease, past the minimum, the air inlet temperature goes above that of the feed water and its exit temperature is now modeled to be the corresponding wet bulb temperature. Thus, in this region, both of the inlet streams contribute energy for the process causing an overall increment of water production which goes up rapidly, as the air contribution goes up and the feed water contribution goes down, and then levels off at the leftmost region as commented before.

Figure 5 was prepared in order to aid the evaluation of air mass flow rate changes on system performance, which is somehow difficult in the two dimensional presentation of Fig. 4. The same information of Fig. 4 is presented in the form of a surface response graph.

As Fig. 4 clearly shows, low air mass flow rates weaken the effect of Q_w/Q_{tot} variations. This is due to the fact that lower air flow rates have lower heat capacities and, therefore, having less sensible heat requirements, permit the use of more energy for the evaporation process. It should also be noted that the efficiency of the system, measured as its capacity to produce water, is greater for low air mass flow rates, which may be explained by the fact that in this analysis the highest overall temperature difference was obtained with the stream of lowest heat capacity.

In order to assert the advantage of heating either the air or the water, attention is now directed to the right and left extremes of the lines of Figs. 4 or 5. As seen there, the maximum water production rate lies somewhere between 1.3 and 1.2 kg/h., so that there is not a definite advantage of heating either of the streams, although it is clear from the results that it is best to apply all heat to only one of the streams. It should also be noted that, as mentioned before, these production rates correspond to fixed water and air solar heater exit temperatures of 100°C and 150°C respectively. Hence, on the basis of the thermodynamic analysis presented here, it is not possible to decide which heating alternative is the best.

The temperature range was selected to investigate solar heating by the simplest possible means of collecting solar energy, which are flat or low efficiency concentrating collectors, but many other simulations have been performed with similar results. Even for flat plate collectors, where typical maximum water and air solar heater exit temperatures are 70°C and 85°C, results show that the maximum production rates are around 1.25 kg/h, and that it does not matter, from the thermodynamic viewpoint, whether the heat input to the system is to the water or the air. This is to be expected since heat-mass transfer mechanisms, which should make the difference were not evaluated.

Accounting for the present design basis, and setting a total daily radiation time of 6 hours, this quantity amounts to a production of 7.5 l/m^2-day, which compares very favorably with the production of common solar still collectors of 3-4 l/m^2-day (Spiegler, 1966), obviously at this stage of the work it is only a good prediction.

CONCLUSIONS

A system to produce distilled water was described and reasons behind system components selection were given. The production of the system was analyzed from the viewpoint of operation strategies and it was found that the best results are obtained by using all the available energy to heat either the air or the water. Analysis were based on mass and energy balances, but temperatures were selected to obtain optimum thermodynamic conditions and inefficiencies introduced by the heat-mass transfer mechanisms were not considered.. Results were obtained through the use of a simulator, which permitted fast and easy evaluation of many possible designs and allowed to estimate a system production of 7.5 kg/m2-day.

REFERENCES

1985 *ASHRAE Handbook Fundamentals* SI Cap.17 Am.Soc. Of Heating, Refrigerating and Air-Conditioning Engineers, Inc. Atlanta

1992 *ASHRAE Handbook HVAC Systems and Equipment* SI Cap.21 Am. Soc. Of Heating, Refrigerating and Air-Conditioning Engineers, Inc. Atlanta

Çengel, Y.A., and Boles, M.A. 1994 *Thermodynamics. An Engineering Approach*. 2nd Edit. McGraw-Hill

Dickinson, W.C., and Cheremisinoff, P.N. Edit. 1980 *Solar Energy Technology Handbook*. Marcel Dekker, Inc.

Kern, D.Q. 1950 *Process Heat Transfer*. McGraw-Hill

Martín-Domínguez, I.R. 1993 *Onset and cessation of nucleate boiling*. Ph.D. Dissertation. University of Windsor. Windsor, Ontario Canada

Spiegler, K.S. 1966 *Principles of Desalination*. Academic Press

Proceedings of the International Solar Energy Conference

SOLAR ENGINEERING 1998

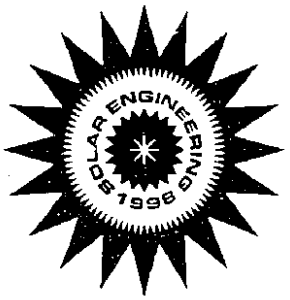

presented at

THE 1998 INTERNATIONAL SOLAR ENERGY CONFERENCE
a part of SOLAR 98: Renewable Energy for the Americas
JUNE 14–17, 1998
ALBUQUERQUE, NEW MEXICO

sponsored by

THE SOLAR ENERGY DIVISION, ASME

edited by

JEFFREY M. MOREHOUSE
UNIVERSITYOF SOUTH CAROLINA

ROY E. HOGAN
SANDIA NATIONAL LABORATORIES

THE AMERICAN SOCIETY OF MECHANICAL ENGINEERS
UNITED ENGINEERING CENTER / 345 EAST 47TH STREET / NEW YORK, NEW YORK 10017

ISBN No. 0-7918-1856-X

Library of Congress Number

FOREWORD

These proceedings contain the 63 peer-reviewed papers that were presented at the 1998 ASME International Solar Energy Conference, which is a component of the jointly hosted SOLAR 98: Renewable Energy for the Americas conference, held in Albuquerque, New Mexico during June 13–18, 1998. This conference is presented by the American Society of Mechanical Engineers — Solar Energy Division, the American Solar Energy Society, and the American Institute of Architects — Committee for the Environment. The overall conference combines the following four conferences:

- ASME International Solar Energy Conference
- 27th ASES Annual Conference
- 23rd National Passive Solar Conference
- AIA Committee on the Environment Symposium

The SOLAR 98 conference was the third time that the organizations listed above held a joint conference. The 63 ASME-sponsored papers in these proceedings were integrated with papers from the other organizations throughout the technical sessions of the overall conference, and grouped by technical session topic. The topics covered by the papers in these proceedings cover advances in solar technologies and building energy conservation including solar heating and cooling, photovoltaics, solar ponds, solar thermal power, desiccant cooling, solar chemistry, building components, and space power systems.

These proceedings represent the results of a year-long process of selection, review, and revision by the 10 ASME Solar Energy Division Technical Committee Chairs and the session organizers. We wish to thank these volunteers, plus the many reviewers, for their time, effort, and expertise in ensuring the continuing quality of the ASME review process. We would also like to express our appreciation to the staff personnel of both ASME and ASES for their support and guidance. Lastly, but most importantly, we thank the authors of these papers for their participation, and hope that this conference provides the interaction and inspiration to sucessfully continue their research and investigations.

Jeffrey H. Morehouse
University of South Carolina

Roy E. Hogan
Sandia National Laboratories